# SUPPLEMENTAL MATERIAL

## Reconstructing source-to-sink systems from detrital zircon core and rim ages

Li Liu, Daniel F. Stockli, Timothy F. Lawton, Jie Xu, Lisa D. Stockli, Majie Fan, and Gregory C. Nadon

## 1. Methods

### 1.1. Mineral Separation

About 1.0- to 1.5-kg outcrop rock material was obtained and used for each sample. Each sample was crushed using jaw crusher and ground using disc mill. Heavy fractions of ground samples were obtained by Wilfley water table and then moved to the oven (40°C) for one day to remove the water. A hand magnet was used before mineral separation in bromoform (2.84 g/cc). After that, Frantz magnetic susceptibility separation was used to remove magnetic minerals with progressive increasing amperage (0.3, 0.5, 1.0, 1.7 A). Finally, methyl iodide (3.3 g/cc) was used as the final step to further separate minerals. All unpolished detrital zircons were sprinkled onto double-sided tape before being depth-profiled using LA-ICP-MS.

### 1.2. Depth-profiling LA-ICP-MS

LA-ICP-MS analyses were conducted using a PhotonMachine Analyte G.2 Excimer laser employing a 30-µm laser spot size at 10 Hz in a large-volume Helex sample cell and a Thermo Element2 ICP-MS. Laser energy density is 2J/cm$^2$. Helium was the carrier gas and was mixed with Argon before entering the ICP-MS. GJ1 was used as the primary reference standard with every five samples analyzed ($^{206}Pb/^{238}U$ age of 601.7 ± 1.3 Ma; Jackson et al., 2004) and Plesovice as a secondary zircon standard with every 30 samples analyzed ($^{206}Pb/^{238}U$ age of 337.1 ± 0.4 Ma; Slama et al., 2008).

Detrital zircon analysis consisted of 4 cleaning shots, 25 seconds of baseline data collection, 30 seconds of laser ablation time, and 30 seconds of washout. The ablation rate is about 0.5 µm/second.

### 1.3. Data Reduction

Interspersed analysis of GJ1 was used to correct the elemental and isotopic fractionation of Pb/U and Pb isotopes. Sample to primary standard (GJ1) measurement ratio is 5:1. Uncertainty from calibration correction of both $^{206}Pb/^{207}Pb$ and $^{206}Pb/^{238}U$ is about 1–2%. Iolite (Igor Pro) and VizualAge (Petrus and Kamber, 2012) were used for age calculation, which is based on ISOPLOT V4 formulas (Ludwig, 2003) from baseline-subtracted intensities. Based on the live U-Pb Concordia diagram, we manually integrate multiple age domains (core and rim) for each analyzed DZ grain. We use $^{206}Pb/^{207}Pb$ and $^{206}Pb/^{238}U$ ages for grains older and younger than 850 Ma, respectively. All grains older than 850 Ma with larger than 20% discordance and grains younger than 850 Ma with more than 10% discordance were discarded, as well as grains with more than 10% analytical error. The DZ U-Pb data is not corrected for common Pb.

### 1.4. Data Plotting

The kernel density estimation (KDE) in Figure 2 and 4 were plotted using detritalPy (Sharman et al., 2018) with 1σ analytical error and band width of 12.

The source code is in this link:

https://github.com/grsharman/detritalPy.

The bivariate KDEs in Figure 3A were plotted using the source code in this link:

https://github.com/cdkortyna/Jupyter-Notebooks.

### 1.5. References


Jackson, S.E., Pearson, N.J., Griffin, W.L., and Belousova, E.A., 2004, The application of laser ablation-inductively coupled plasma-mass spectrometry to in situ U–Pb zircon geochronology: Chemical Geology, v. 211, p. 47–69, https://doi.org/10.1016/j.chemgeo.2004.06.017.

Ludwig, K.R., 2003, Isoplot/Ex 3.00: A geochronological toolkit for Microsoft Excel: Berkeley Geochronology Center Special Publication 4.

Petrus, J.A., and Kamber, B.S., 2012, VizualAge: A Novel Approach to Laser Ablation ICP-MS U-Pb Geochronology Data Reduction: Geostandards and Geoanalytical Research, v. 36, p. 247–270. https://doi.org/10.1111/j.1751-908X.2012.00158.x.

Sharman, G.R., Sharman, J.P., and Sylvester, Z., 2018, detritalPy: A Python-based toolset for visualizing and analysing detrital geo-thermochronologic data: The Depositional Record, v. 4, p. 202–215, https://doi.org/10.1002/dep2.45.

Sláma, J., Košler, J., Condon, D. J., Crowley, J.L., Gerdes, A., Hanchar, J.M., Horstwood, M.S.A., Morris, G.A., Nasdala, L., Norberg, N., Schaltegger, U., Schoene, B., Tubrett, M.N., and Whitehouse, M.J., 2008, Plešovice zircon — A new natural reference material for U–Pb and Hf isotopic microanalysis: Chemical Geology, v. 249, p. 135, https://doi.org/10.1016/j.chemgeo.2007.11.005.

## 2. Figure S1

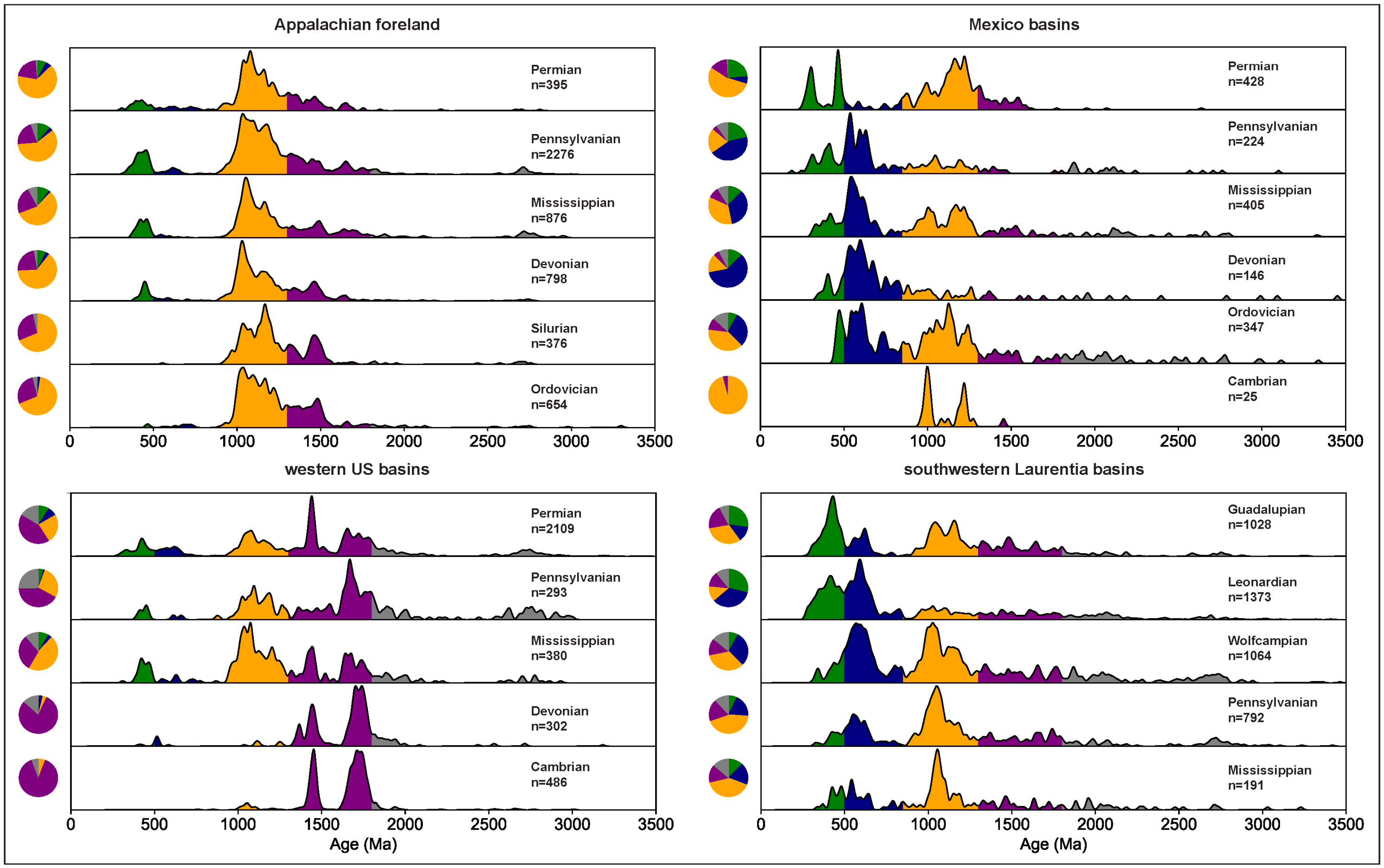

Appalachian foreland
Permian
n=395
Pennsylvanian
n=2276
Mississippian
n=876
Devonian
n=798
Silurian
n=376
Ordovician
n=654
Mexico basins
Permian
n=428
Pennsylvanian
n=224
Mississippian
n=405
Devonian
n=146
Ordovician
n=347
Cambrian
n=25
western US basins
Permian
n=2109
Pennsylvanian
n=293
Mississippian
n=380
Devonian
n=302
Cambrian
n=486
southwestern Laurentia basins
Guadalupian
n=1028
Leonardian
n=1373
Wolfcampian
n=1064
Pennsylvanian
n=792
Mississippian
n=191
0
500
1000
1500
2000
2500
3000
3500
Age (Ma)

Appalachian foreland are mainly in the middle and south of the basin and some DZ in Ordovician may derive from pre-Taconic passive margin deposit. Guadalupian was shown in International Chronostratigraphic Chart, ca. 273.01–259.51 Ma. Leonardian is North American Stage, ca. 280–271 Ma, approximately corresponding to Kungurian, 283.5–273.01 Ma. Wolfcampian is North American Stage, ca. 300–280 Ma, approximately corresponding to Asselian, Sakmarian, and Artinskian Stages, ca. 298.9–283.5 Ma (Cohen et al., 2013; updated). See compiled data in Data Repository File DR3. The timeframe of these colors and related interpretations are shown in Figure 2.

## 2.2. Data Source of Figure S1.

| **Period** | **Region** | **References** |
|---|---|---|
| *Appalachian Foreland* | | |
| Permian | Appalachian foreland | (Becker et al., 2006; Thomas et al., 2017) |
| Pennsylvanian | Appalachian foreland | (Becker et al., 2005; Dodson, 2008; Eriksson et al., 2004; Gray and Zeitler, 1997; Thomas et al., 2004) |
| Mississippian | Appalachian foreland | (Park et al., 2010; Thomas et al., 2017) |
| Devonian | Appalachian foreland | (Eriksson et al., 2004; McLennan et al., 2001; Park et al., 2010; Thomas et al., 2017) |
| Silurian | Appalachian foreland | (Eriksson et al., 2004; Gray and Zeitler, 1997; McLennan et al., 2001; Park et al., 2010) |
| Ordovician | Appalachian foreland | (Eriksson et al., 2004; McLennan et al., 2001; Park et al., 2010; Thomas et al., 2017) |
| *Mexico* | | |
| Triassic | Central Mexico | (Ortega-Flores et al., 2014) |
| Permian | Acatlan complex | (Keppie et al., 2004; Sánchez-Zavala et al., 2004; Talavera-Mendoza et al., 2005) |
| Pennsylvanian | Oaxaca, Maya Block, Acatlan complex | (Gillis et al., 2005; Talavera-Mendoza et al., 2005; Weber et al., 2006) |
| Mississippian | Oaxaca, Chiapas, Acatlan complex | (Gillis et al., 2005; Grodzicki et al., 2008; Weber et al., 2009) |
| Devonian | Acatlan complex | (Talavera-Mendoza et al., 2005) |
| Ordovician | Northwest Mexico, Acatlan Complex | (Gillis et al., 2005; Talavera-Mendoza et al., 2005) |
| Cambrian | Oaxaca | (Gillis et al., 2005) |

| | | |
|---|---|---|
| *Western United States* | | |
| Triassic | Colorado Plateau, Grand Canyon | (Dickinson and Gehrels, 2008) |
| Permian | Paradox Basin, Grand Canyon | (Dickinson and Gehrels, 2003; Gehrels et al., 2011; Lawton et al., 2015) |
| Pennsylvanian | Grand Canyon | (Gehrels et al., 2011) |
| Mississippian | Grand Canyon | (Gehrels et al., 2011) |
| Devonian | Grand Canyon | (Gehrels et al., 2011) |
| Cambrian | Grand Canyon | (Gehrels et al., 2011) |
| *Southwestern Laurentia* | | |
| Guadalupian Stage | Permian Basin | (Soreghan and Soreghan, 2013; Xie et al., 2019) |
| Leonardian Stage | Permian Basin | (Liu and Stockli, 2020) |
| Wolfcampian Stage | Permian Basin | (Liu and Stockli, 2020) |
| Pennsylvanian | Fort Worth Basin | (Alsalem et al., 2018) |
| Mississippian | Ouachita Orogen | (McGuire, 2017) |

### 2.3. References of Figure S1.

Alsalem, O.B., Fan, M., Zamora, J., Xie, X., Griffin, W.R., 2018. Paleozoic sediment dispersal before and during the collision between Laurentia and Gondwana in the Fort Worth Basin, USA: Geosphere, v. 14, p. 325–342, https://doi.org/10.1130/GES01480.1.

Becker, T.P., Thomas, W.A., Gehrels, G.E., 2006. Linking late Paleozoic sedimentary provenance in the Appalachian Basin to the history of Alleghanian deformation: American Journal of Science, v. 306, p. 777–798, https://doi.org/10.2475/10.2006.01.

Becker, T.P., Thomas, W.A., Samson, S.D., Gehrels, G.E., 2005. Detrital zircon evidence of Laurentian crustal dominance in the lower Pennsylvanian deposits of the Alleghanian clastic wedge in eastern North America: Sedimentary Geology, v. 182, p. 59–86, https://doi.org/10.1016/j.sedgeo.2005.07.014.

Cohen, K.M., Finney, S.C., Gibbard, P.L., and Fan, J.-X., 2013; updated, The ICS International Chronostratigraphic Chart: Episodes, v. 36, p. 199–204.

Dickinson, W.R., Gehrels, G.E., 2003. U–Pb ages of detrital zircons from Permian and Jurassic eolian sandstones of the Colorado Plateau, USA: paleogeographic implications: Sedimentary Geology, v. 163, p. 29–66, https://doi.org/10.1016/S0037-0738(03)00158-1.

Dickinson, W.R., Gehrels, G.E., 2008. U-Pb ages of detrital zircons in relation to paleogeography: Triassic paleodrainage networks and sediment dispersal across southwest Laurentia: Journal of Sedimentary Research, v. 78, p. 745–764, https://doi.org/10.2110/jsr.2008.088.

Dodson, S.A., 2008. Petrographic and geochronologic provenance analysis of upper Pennsylvanian fluvial sandstones of the Conemaugh and Monongahela Groups, Athens County, Ohio: Master Thesis, Ohio University, Athens, Ohio, USA, 86 p.

Eriksson, Kenneth A., Ian H. Campbell, J. Michael Palin, Charlotte M. Allen, Barbara Bock, 2004. Evidence for multiple recycling in Neoproterozoic through Pennsylvanian sedimentary rocks of the central Appalachian basin: The Journal of Geology, v. 112, p. 261–276, https://doi.org/10.1086/382758.

Gehrels, G.E., Blakey, R., Karlstrom, K.E., Timmons, J.M., Dickinson, B., Pecha, M., 2011. Detrital zircon U-Pb geochronology of Paleozoic strata in the Grand Canyon, Arizona: Lithosphere, v. 3, p. 183–200, https://doi.org/10.1130/l121.1.

Gillis, R.J., Gehrels, G.E., Ruiz, J., Flores de Dios Gonzaléz, L.A., 2005. Detrital zircon provenance of Cambrian–Ordovician and Carboniferous strata of the Oaxaca terrane, southern Mexico: Sedimentary Geology, v. 182, p. 87–100, https://doi.org/10.1016/j.sedgeo.2005.07.013.

Gray, M.B., Zeitler, P.K., 1997. Comparison of clastic wedge provenance in the Appalachian foreland using U/Pb ages of detrital zircons: Tectonics, v. 16, p. 151–160, https://doi.org/10.1029/96tc02911.

Grodzicki, K.R., Nance, R.D., Keppie, J.D., Dostal, J., Murphy, J.B., 2008. Structural, geochemical and geochronological analysis of metasedimentary and metavolcanic rocks of the Coatlaco area, Acatlán Complex, southern Mexico: Tectonophysics, v. 461, p. 311–323, https://doi.org/10.1016/j.tecto.2008.01.016.

Keppie, J.D., Sandberg, C.A., Miller, B.V., Sánchez-Zavala, J.L., Nance, R.D., Poole, F.G., 2004. Implications of latest Pennsylvanian to middle Permian paleontological and U-Pb SHRIMP data from the Tecomate Formation to re-dating tectonothermal events in the

Acatlán Complex, southern Mexico: International Geology Review, v. 46, p. 745–753, https://doi.org/10.2747/0020-6814.46.8.745.

Lawton, T.F., Buller, C.D., Parr, T.R., 2015. Provenance of a Permian erg on the western margin of Pangea: Depositional system of the Kungurian (late Leonardian) Castle Valley and White Rim sandstones and subjacent Cutler Group, Paradox Basin, Utah, USA: Geosphere, v. 11, p. 1475–1506, https://doi.org/10.1130/ges01174.1.

Liu, L., Stockli, D.F., 2020. U-Pb ages of detrital zircons in lower Permian sandstone and siltstone of the Permian Basin, west Texas, USA: Evidence of dominant Gondwanan and peri-Gondwanan sediment input to Laurentia: Geological Society of America Bulletin, v. 132, p. 245–262, https://doi.org/10.1130/b35119.1.

McGuire, P.R., 2017. U-Pb Detrital zircon signature of the Ouachita orogenic belt: Master Thesis, Texas Christian University, Fort Worth, Texas, USA, p. 88.

McLennan, S., Bock, B., Compston, W., Hemming, S., McDaniel, D., 2001. Detrital zircon geochronology of Taconian and Acadian foreland sedimentary rocks in New England: Journal of Sedimentary Research, v. 71, p. 305–317, https://doi.org/10.1306/072600710305.

Ortega-Flores, B., Solari, L., Lawton, T.F., Ortega-Obregón, C., 2014. Detrital-zircon record of major Middle Triassic–Early Cretaceous provenance shift, central Mexico: Demise of Gondwanan continental fluvial systems and onset of back-arc volcanism and sedimentation: International Geology Review, v. 56, p. 237–261, https://doi.org/10.1080/00206814.2013.844313.

Park, H., L. Barbeau, D., Rickenbaker, A., Bachmann-Krug, D., Gehrels, G., 2010. Application of foreland basin detrital-zircon geochronology to the reconstruction of the southern and central Appalachian orogen: The Journal of Geology, v. 118, p. 23–44, https://doi.org/10.1086/648400.

Sánchez-Zavala, J.L., Ortega-Gutiérrez, F., Keppie, J.D., Jenner, G.A., Belousova, E., Maciás-Romo, C., 2004. Ordovician and Mesoproterozoic zircons from the Tecomate Formation and Esperanza Granitoids, Acatlán Complex, southern Mexico: Local provenance in the Acatlán and Oaxacan Complexes: International Geology Review, v. 46, p. 1005–1021, https://doi.org/10.2747/0020-6814.46.11.1005.

Soreghan, G.S., and Soreghan, M.J., 2013, Tracing clastic delivery to the Permian Delaware Basin, U.S.A.: Implications for paleogeography and circulation in westernmost equatorial, Pangea:: Journal of Sedimentary Research, v. 83, p. 786–802, https://doi.org/710.2110/jsr.2013.2163.

Talavera-Mendoza, O., Ruiz, J., Gehrels, G.E., Meza-Figueroa, D.M., Vega-Granillo, R., Campa-Uranga, M.F., 2005. U–Pb geochronology of the Acatlán Complex and implications for the Paleozoic paleogeography and tectonic evolution of southern Mexico: Earth and Planetary Science Letters, v. 235, p. 682–699, https://doi.org/10.1016/j.epsl.2005.04.013.

Thomas, W.A., Becker, T.P., Samson, S.D., Hamilton, M.A., 2004. Detrital zircon evidence of a recycled orogenic foreland provenance for Alleghanian clastic-wedge sandstones: The Journal of Geology, v. 112, p. 23–37, https://doi.org/10.1086/379690.

Thomas, W.A., Gehrels, G.E., Greb, S.F., Nadon, G.C., Satkoski, A.M., Romero, M.C., 2017. Detrital zircons and sediment dispersal in the Appalachian foreland: Geosphere, v. 13, p. 2206–2230, https://doi.org/10.1130/ges01525.1.

Weber, B., Schaaf, P., Valencia, V.A., Iriondo, A., Ortega-Gutiérrez, F., 2006. Provenance ages of late Paleozoic sandstones (Santa Rosa Formation) from the Maya Block, SE México: implications on the tectonic evolution of western Pangea: Revista mexicana de ciencias geológicas, v. 23, p. 262–276.

Weber, B., Valencia, V.A., Schaaf, P., Gutiérrez, F.O., 2009. Detrital zircon ages from the Lower Santa Rosa Formation, Chiapas: implications on regional Paleozoic stratigraphy: Revista Mexicana de Ciencias Geológicas, v. 26, p. 260–276.

Xie, X., Anthony, J.M., Busbey, A.B., 2019. Provenance of Permian Delaware Mountain Group, central and southern Delaware Basin, and implications of sediment dispersal pathway near the southwestern terminus of Pangea: International Geology Review, v. 61, p. 361–380, https://doi.org/10.1080/00206814.2018.1425925.